Vacuum Ultraviolet Negative Photoion Spectroscopy of Chloroform

ARTICLE *in* THE JOURNAL OF PHYSICAL CHEMISTRY A · APRIL 2011

Impact Factor: 2.69 · DOI: 10.1021/jp2000927 · Source: PubMed

7 AUTHORS, INCLUDING:

Shan Xi Tian
University of Science and Technology of China
88 PUBLICATIONS **713** CITATIONS

SEE PROFILE

THE JOURNAL OF PHYSICAL CHEMISTRY A

ARTICLE

pubs.acs.org/JPCA

Vacuum Ultraviolet Negative Photoion Spectroscopy of Chloroform

Liu-Li Chen,[†] Yun-Feng Xu,[†] Qiang Feng,[†] Shan Xi Tian,[*,†] Fu-Yi Liu,[‡] Xiao-Bin Shan,[‡] and Liu-Si Sheng[‡]

[†]Hefei National Laboratory for Physical Sciences at the Microscale and Department of Chemical Physics, University of Science and Technology of China, Hefei, Anhui 230026, China

[‡]National Synchrotron Radiation Laboratory, University of Science and Technology of China, Hefei, Anhui 230029, China

ABSTRACT: Negative ions Cl^-, Cl_2^-, CCl^-, $CHCl^-$, and CCl_2^- are observed in vacuum-ultraviolet ion-pair photodissociations of chloroform (CCl_3H) using the Hefei synchrotron radiation facility, and their ion production efficiency curves are recorded in the photon energy range of 10.00−21.50 eV. Two similar spectra of the isotope anions $^{35}Cl^-$ and $^{37}Cl^-$ indicate the following: Besides the strong bands corresponding to the electron transitions from valence to Rydberg orbitals converging to the ionic states, some additional peaks can be assigned with the energetically accessible multibody fragmentations; a distinct peak at photon energy 14.55 eV may be due to a cascade process (namely, the Cl_2 neutral fragment at the highly excited state $D'2^3\Pi_g$ may be produced in the photodissociation of CCl_3H, and then the Cl^- anions are produced in the pulsed-field induced ion-pair dissociations of Cl_2 ($D'2^3\Pi_g$)); two vibrational excitation progressions, $n\nu_2^+$ and $n\nu_2^+ + \nu_3^+$, and $n\nu_4^+$ and $n\nu_4^+ + \nu_2^+$, are observed around $\tilde{C}\ ^2E$ and $\tilde{D}\ ^2E$ ionic states, respectively. The enthalpies of the multibody fragmentations to Cl_2^-, CCl^-, $CHCl^-$, and CCl_2^- are calculated with the thermochemistry data available in the literature, and these multibody ion-pair dissociation pathways are tentatively assigned in the respective anion production spectra.

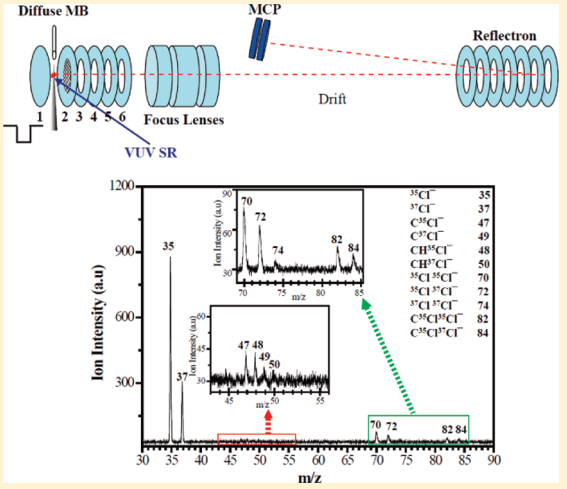

1. INTRODUCTION

Positive ion−negative ion pair (simply noted as ion-pair) photodissociation, established as a novel unimolecular process, occurs rather commonly in the wide energy range (from several to hundreds of electronvolts)[1−3] and for a variety of molecules.[1−10] When ion-pair predissociation states are coupled with the vibrational states of a certain valence excited state or Rydberg state, correspondingly, ion-pair anion efficiency spectra (IPAES) exhibit the discrete structures that can be assigned with Rydberg-like or vibrational-excited series.[1−10] On the other hand, in the photoexcitation when the target molecule is vertically promoted to the repulsive wall of the potential energy surfaces of the ion-pair states, the structureless band will be presented in IPAES due to the direct fast ion-pair dissociations. For polyatomic molecules, the multibody fragmentation is also frequently observed above the molecular ionization threshold. When the ion-pair states are embedded in the ionization and dissociation continua, the cross-sections of ion-pair dissociation are usually much smaller (on the order of 0.1% or less of the total photoabsorption cross-sections of a polyatomic molecule[1]) due to decaying competitions with the other dominant channels such as direct or autoionizations, dissociative ionizations, neutral fragmentations, and light emission. Thus, it is difficult to access the experimental studies of the ion-pair dissociation, not only due to its minor contribution to the decaying channels of the molecular excited states but also the requirement of an energy-broad light source. It is appealing that such demanding is satisfied well with the high sensitivity of the state-of-art time-of-flight (TOF) mass spectrometry and the broad-band tunability of synchrotron radiation.[3−9,19−23]

In this work, we report an ion-pair photodissociation study of chloroform (CCl_3H). As a basic and widely used organic compound, CCl_3H is the main natural and anthropogenic source of active chlorine[11,12] and should be responsible for the depletion of the ozone layer in the stratosphere and for the greenhouse effects. A lot of studies on this molecule have been carried out over the past several decades using various techniques.[13−20] Among these studies, CCl_3H was studied by photoabsorption spectroscopy in the 105−220 nm region.[14] Dissociative electron attachment (DEA) to CCl_3H was studied in the electron energy range of 0−25 eV.[15] The photoionization yields of CCl_3H have been measured in the 10.0−13.5 eV energy range.[16] The He(I) and He(II) photoelectron spectra of CCl_3H revealed its orbital structures and provided the vertical ionization potentials (IP_vs).[17,18] Vacuum-ultraviolet (vacuum-UV) fluorescence spectroscopy and threshold photoelectron−photoion coincidence (TPEPICO) spectroscopy studies have been performed by Seccombe et al. in the photon energy range of 8−30 eV.[20] Here the negative ion fragments, Cl^-, Cl_2^-, CCl^-, $CHCl^-$, and

Received: January 5, 2011
Revised: March 14, 2011
Published: April 01, 2011

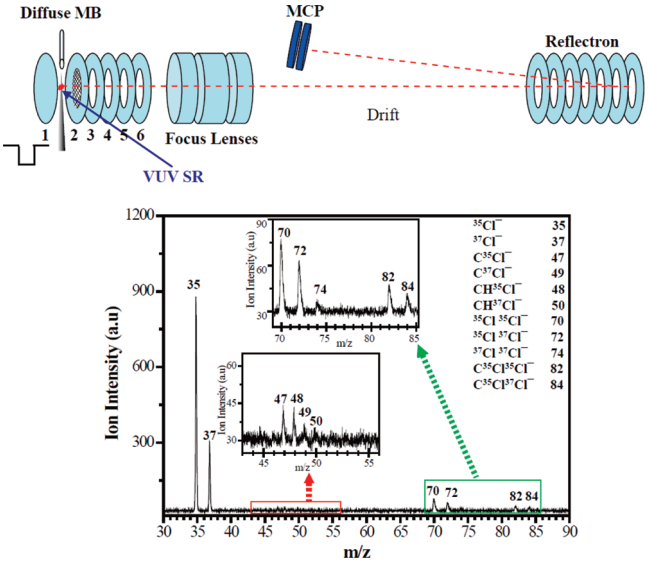

Figure 1. Our homemade reflectron time-of-flight mass spectrometer and negative photoion mass spectrum at the photon energy of 20.36 eV.

CCl_2^-, produced in the vacuum-UV ion-pair photodissociations of CCl_3H, have been detected, and their productions are recorded as a function of photon energy in the range of 10.00−21.50 eV using the Hefei synchrotron radiation facility. To the best of our knowledge, there are no reports prior to this work on the ion-pair photodissociations of CCl_3H.

2. EXPERIMENTAL METHODS AND THERMOCHEMISTRY CALCULATIONS

The IPAES of Cl^- and the other negative ion fragments were recorded at the atomic and molecular physics end-station of the national synchrotron radiation facility at Hefei, China. The apparatus has been described in detail elsewhere.[9,22,23] Its reliability and sensitivity have been proved by comparison of our IPAES of CO_2 with that available in the literature.[22,23] As shown in Figure 1 (upper panel), the vacuum-UV photon beam was monochromatized with the undulator-based spherical gratings (made by Horiba Jobin Yvon) and then focused onto the photoionization region. A diffuse molecular beam was introduced with a stainless steel tube with a diameter of 0.5 mm. The anionic fragments were collected with a homemade reflectron TOF mass spectrometer which is installed perpendicularly to the plane containing the molecular beam and the photon beam. The total length of flight of the ions is 1400 mm. Packets of anions were pushed periodically from the ionization region by a pulsed repeller (lens 1) with a voltage of −165 V (1.5−2.0 μs pulse width and 18 000 Hz repetition) into an acceleration region, wherein they were accelerated by an electrostatic field of 1000 V. But even in the absence of the pulsed repeller voltage, when no potential gradient exists in the extraction region, some ions enter the acceleration region due to the existence of leakage fields which reduces the signal-to-noise ratio. The more serious problem in the IPAES experiments is the serious background noise arising from an abundant of photoionization electrons. Thus, the low DC negative voltages, typically of −0.04 and −0.45 V, were added on lenses 1 and 2 (its mesh-covered aperture is of diameter 20 mm), respectively, to efficiently kick out the photoelectrons but maintain the heavy negative ions. The pulsed anion beam was focused (900 V) and transferred through drift area (floated on 1000 V) and then reflected by the retarding lenses (the last lens was on −460 V). At last the anions were detected with two zigzag stacking microchannel plates.

The wavelength of the vacuum-UV beam was calibrated and the energy resolution ($E/\Delta E$ = 5000) was determined before the present experiments. The energy scanning step and the signal accumulation time at each step were typically 0.02 eV and 60 s, respectively. To normalize the anion signals, the photon flux was monitored with a silicon photodiode (SXUV-100, International Radiation Detectors, Inc.). The commercial sample CCl_3H (purity > 99.9%) was used without further purification. When the photon energy is higher than the molecular ionization threshold (i.e., the lowest adiabatic ionization potential, IP_a), the anionic fragments may be produced through the dissociative photoelectron attachments to the parent molecule.[15] This pathway will interfere with the anion signals observed in the present experiments. If the sample intensities in the reaction areas are low enough, the photoelectron attachments as the secondary reactions can be diminished and such interferences can be ruled out.

For many polyatomic molecules, when suitable assumptions are made about the nature of the accompanying cationic and neutral fragment(s), a calculated threshold energy is a lower limit to the experimental appearing energy (AE) of an anion.[1] To access the ion-pair dissociation channel, for example, the diatomic molecule AB [$AB + h\nu \rightarrow A^+ + B^-$], its energetic threshold $E_{threshold}$ is determined by

$$E_{threshold} = D_0(A^+ - B) + IP_a(AB) - EA(B) \leq AE(B^-) \quad (1)$$

where D_0 is the dissociation energy of $(AB)^+$ (to A^+ and B), $IP_a(AB)$ is the IP_a value of AB, and EA(B) is the electron affinity of B. When EA(B) > $D_0(A^+-B)$, B^- can be produced at the photon energy less than the ionization threshold, i.e., $IP_a(AB)$. If the dynamic energetic barrier of the ion-pair dissociation is not considered, here the thermochemical energies, i.e., dissociation energies, for the anionic fragment yields can be estimated. Furthermore, two assumptions are made when enthalpies of appropriate dissociation reactions (or unimolecular reactions) are estimated at 298 K (AE_{298}):[6,7,21] The corrections to the AE_{298} value when it is approximated to be $\Delta_r H^\circ_{298}$ are typically only 0.05−0.15 eV [24] and can be ignored to some extent; the effects of entropy are disregarded, which leads to the more negative $\Delta_r G^\circ_{298}$ with respect to the calculated $\Delta_r H^\circ_{298}$ values.

For the ion-pair photodissociations of CCl_3H, since the room-temperature diffuse beam was employed in this work, the formation enthalpy $\Delta_f H^\circ$ = −1.068 34 eV (−103.117 kJ/mol) at 298 K of CCl_3H and the enthalpies of the daughter ions and the neutral fragments (at 0 K) at the ground states given in the JANAF tables[25] were used to calculate the ion-pair dissociation energies. Here the internal energies of the daughter ions and fragments were excluded. When the enthalpy values were not available, the data for cations, CCl^+, $CClH^+$, CCl_2^+, and $CHCl_2^+$, at 298 K from Lias et al.[26] were used. Note that $\Delta_f H^\circ$ values of Cl_2^+ and HCl^+ were obtained indirectly using the IP_a values of Cl_2 (11.4864 ± 0.00012 eV) [27] and HCl (12.745(2) eV) [28] and the 0 K $\Delta_f H^\circ$ values of Cl_2 and HCl.[25] The EA values of 2.50 ± 0.20 eV (Cl_2),[29] 1.590 ± 0.070 eV (CCl_2),[30] 0.89 ± 0.2 eV (CCl),[31] and 1.2100 ± 0.0050 eV (CClH)[32] were used in the energetic calculations for Cl_2^-, CCl_2^-, CCl^-, and $CClH^-$, respectively. The excited-state energies of neutral

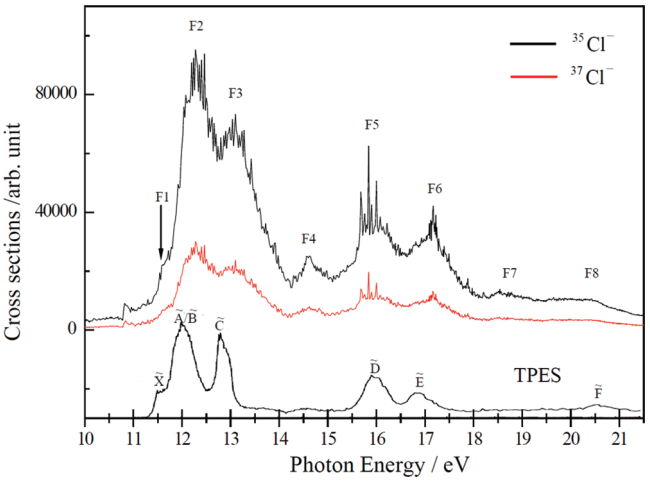

Figure 2. Anion yield spectra for $^{35}Cl^-$ and $^{37}Cl^-$ and the threshold photoelectron spectrum (TPES) of CCl_3H. Reproduced with permission from ref 20. Copyright 2000 Royal Society of Chemistry.

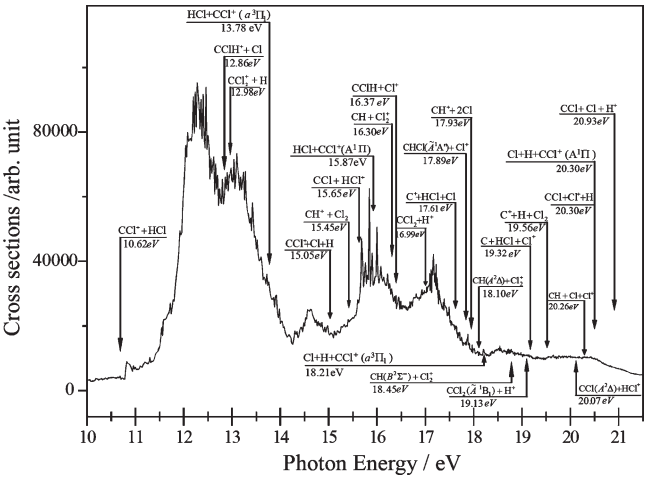

Figure 3. Multibody fragmentations tentatively assigned in the spectrum of Cl^-.

fragments CClH, CCl_2, and CCl^+ were taken from refs 33 and 34. For some specific channels, the thermochemical data from refs 19 and 20 together with the EA (3.6144 eV) [35] of Cl and the IP_a values of Cl_2 [27] and HCl [28] were used in the calculations.

3. RESULTS AND DISCUSSION

We found 11 anionic fragments in the mass spectra at the photon energy around 20.36 eV, see Figure 1, in which the minor isotopic anions were observed but the signals were quite low. Therefore, only the IPAES of $^{35}Cl^-$ and $^{70}Cl_2^-$ were discussed in the following text. In the DEA study of CCl_3H, 10 different anionic fragments were observed.[15] In that work, the intensities of CCl_2^- species are about 200 and 50 times higher than those of $CHCl^-$ and Cl_2^-.[15] Here, the intensities of Cl_2^- are a little higher than those of CCl_2^-, while the intensities of $CHCl^-$ and CCl_2^- are comparable. This indicates again that the DEA interference to the IPAES has been successfully removed.

IPAES of Cl^-. The $^{35}Cl^-$ and $^{37}Cl^-$ total ion yield curves in the photon energy range of 10.00−21.50 eV are depicted in Figure 2. The threshold photoelectron spectrum (TPES) available in ref 20 is also shown for comparison. Two IPAES show the same features; moreover, the ion intensity ratio of $^{35}Cl^-$:$^{37}Cl^-$ in the whole energy range approximately equals the natural isotope abundance ratio ^{35}Cl:^{37}Cl = 3:1. Eight bands in the anionic production curves are assigned as F1−F8. F1−F3, F5, F6, and F8 may be closely related to the electron transitions from valence to Rydberg orbitals that converge to seven valence ionic states, $\tilde{X}$, $\tilde{A}/\tilde{B}$, $\tilde{C}$, $\tilde{D}$, $\tilde{E}$, and $\tilde{F}$, respectively. The IP_v values for $\tilde{X}\ ^2A_2$, $\tilde{A}\ ^2A_1$/$\tilde{B}\ ^2E$, $\tilde{C}\ ^2E$, $\tilde{D}\ ^2E$, $\tilde{E}\ ^2A_1$, and $\tilde{F}\ ^2A_1$ were experimentally determined to be 11.51, 12.02, 12.78, 15.95, 16.84, and 20.65 eV, respectively.[20] Besides these six bands, two additional bands, F4 and F7, are observed in Figure 2, but they are absent in the photoelectron spectra.[17,18,20] This implies that they cannot be directly related to the valence electron transitions of CCl_3H. As discussed in the following text, they basically resulted from the multibody fragmentations and novel cascade dissociations.

At the photon energies below the lowest IP_v (here assigned as the $\tilde{X}\ ^2A_2$ state), a series of Rydberg transitions were observed in the photoabsorption spectra.[14] According to the assignments by Lee and Suto,[14] there were some series of Rydberg−vibrational progressions. In Figures 2 and 3, a distinct onset of the Cl^- curve at 10.80 eV (at the low-energy end of band F1) happens to be close in energy to an electron transition to the Rydberg−vibrational excited state Cl(5p) $9\nu_3^+$,[14] where the vibrational mode ν_3^+ is CCl_3 symmetrical deformation of the ion core (CCl_3H^+) at the ground state. It is interesting that a small peak at 10.7 eV was observed in the fluorescence excitation spectrum and assigned as the electron transitions from the Cl nonbonding orbital.[19] The previous study on the electron structures of CCl_3H indicates that the character of $1a_2$ orbital (the highest occupied molecular orbital) is purely of Cl 3p lone-pair orbital.[36] Thus, the Rydberg series including the Rydberg−vibrational excitation to 5p ($9\nu_3^+$) at 10.80 eV should converge to $\tilde{X}\ ^2A_2$ (IP_v = 11.51 eV [20]), rather than the ^2E ionic state.[14] On the other hand, the onset of Cl^- signals at 10.80 eV may be related to such a process, $CCl_3H + h\nu \rightarrow CCl^+ + HCl + Cl^-$ ($E_{threshold}$ = 10.62 eV). As assigned in Figure 3 and the multibody fragmentations listed in Table 1, the energetic threshold to produce Cl^- is estimated to be as low as 7.89 eV [$CCl_3H + h\nu \rightarrow CCl_2H^+ + Cl^-$], but this threshold cannot be experimentally determined due to too poor signal strength at energies less than 10.0 eV. Moreover, the ion-pair dissociations via the photoexcitations of the thermally vibrational exited CCl_3H may somewhat contribute to the weak signals of Cl^- in the energy range of 10.00−10.80 eV, i.e., as the hot band of the IPAES, because the thermal diffuse beam is used in the experiments. Due to almost the same IP_v values of $\tilde{A}\ ^2A_1$ and $\tilde{B}\ ^2E$ and the complicated structures (such as Rydberg and vibrational excitations, Jahn−Teller, and spin−orbital splits around the $\tilde{B}\ ^2E$ state) in the photoexcitation and photoionization spectra,[17,18,20] the band F2 (11.5−12.2 eV) is hardly resolved.

In the energy range of 12.20−12.80 eV of the F3 band, there are some fine structures. The IP_v of $\tilde{C}\ ^2E$ was determined as 12.78 eV.[20] The corresponding orbital 3e is a degenerate orbital and basically consists of Cl 3p orbitals. In Figure 4a, two sets of vibrational progressions, $n\nu_2^+$ and $n\nu_2^+ + \nu_3^+$, accompanying the electron promotion from the 3e orbital are tentatively assigned with references of the high-resolution photoelectron spectra of CCl_3F (in the same symmetry C_{3v} as CCl_3H).[37] The average values of the ν_2^+ and ν_3^+ frequencies of the ion core CCl_3H^+ at the ^2E excited state are estimated to be 90 and 40 meV, respectively. They are close to the corresponding ν_2 (84.3

Table 1. Energetics of Ion-Pair Dissociation Channels and Vertical Ionization Potentials of $CHCl_3$

neutral/parent ion	ion-pair dissociation channel	dissociation energy/eV	vertical ionization potential/eV
	$Cl^- + CCl + Cl + H^+$	20.93 [a]	
	$Cl^- + CCl + H + Cl^+$	20.30 [a]	
	$Cl^- + Cl + H + CCl^+(A\ ^1\Pi)$	20.30 [a]	
	$Cl^- + CH + Cl + Cl^+$	20.26 [a]	
	$Cl^- + CCl(A\ ^2\Delta) + HCl^+$	20.07 [b]	
$CCl_3H^+\ \tilde{F}\ ^2A_1$			19.8,[c] 20.65,[d] 20.8[e]
	$Cl^- + H + Cl_2 + C^+$	19.56 [a]	
	$Cl^- + C + HCl + Cl^+$	19.32 [a]	
	$Cl^- + CCl_2(\tilde{A}\ ^1B_1) + H^+$	19.13 [a]	
	$Cl^- + CH(B\ ^2\Sigma^-) + Cl_2^+$	18.45 [b]	
	$Cl^- + Cl + H + CCl^+(a^3\Pi_1)$	18.21 [a]	
	$Cl^- + CH(A\ ^2\Delta) + Cl_2^+$	18.10 [b]	
	$Cl^- + 2Cl + CH^+$	17.93,[a] 17.93 [f]	
	$Cl^- + CClH(\tilde{A}\ ^1A'') + Cl^+$	17.89 [a]	
	$Cl^- + HCl + Cl + C^+$	17.61 [a]	
	$Cl^- + CCl_2 + H^+$	16.99 [a]	
$CCl_3H^+\ \tilde{E}\ ^2A_1$			16.96,[c] 16.84,[d] 17.0[e]
	$Cl^- + CClH + Cl^+$	16.37 [a]	
	$Cl^- + CH + Cl_2^+$	16.30 [a]	
$CCl_3H^+\ \tilde{D}\ ^2E$			15.99,[c] 15.95,[d] 16.0[e]
	$Cl^- + HCl + CCl^+(A\ ^1\Pi)$	15.87 [a]	
	$Cl^- + CCl + HCl^+$	15.65 [a]	
	$Cl^- + Cl_2 + CH^+$	15.45,[a] 15.46 [f]	
	$Cl^- + Cl + H + CCl^+$	15.05,[a] 15.00 [f]	
	$Cl^- + HCl + CCl^+(a^3\Pi_1)$	13.78 [a]	
	$Cl^- + H + CCl_2^+$	12.98,[a] 12.93 [f]	
$CCl_3H^+\ \tilde{C}\ ^2E$			12.85,[c] 12.78,[d] 12.9[e]
	$Cl^- + Cl + CClH^+$	12.86,[a] 12.81 [f]	
$CCl_3H^+\ \tilde{B}\ ^2E$			12.01,[c] 12.02,[d] 12.0[e]
$CCl_3H^+\ \tilde{A}\ ^2A_1$			11.91,[c] 12.02,[d] 12.0[e]
$CCl_3H^+\ \tilde{X}\ ^2A_2$			11.48,[c] 11.51,[d] 11.5[e]
	$Cl^- + HCl + CCl^+$	10.62,[a] 10.57 [f]	
	$Cl^- + CCl_2H^+$	7.89,[a] 7.79 [f]	
$CCl_3H\ \tilde{X}\ ^1A_1$			0.00

[a] Calculated in this work. [b] Estimated using the thermochemical data from ref 19. [c] Cited from ref 17. [d] Cited from ref 20. [e] Cited from ref 18. [f] Estimated using the thermochemical data from ref 20.

meV, CCl_3 symmetrical stretching mode) and ν_3 (45 meV) frequencies of the ground-state CCl_3H.[38] Due to the promotion of the Cl 3p electron in 3e orbital, these two vibration modes related to C−Cl bonds are activated. Such nonadiabatic processes, i.e., the vibrational−electron coexcitations, are demonstrated to be coupled with the ion-pair dissociations. In a similar scenario, another two sets of vibrational progressions, $n\nu_4^+$ and $n\nu_4^+ + \nu_2^+$, accompanying the electron promotion from the 2e orbital (with C−H bonding character and corresponding to the $\tilde{D}\ ^2E$ state) are tentatively assigned to the more distinct peaks of band F5 in the energy range of 15.50−16.50 eV, as shown in Figure 4b. The average frequencies ν_4^+ of 140 meV (the corresponding value of the neutral is 151 meV, C−H bending mode[38]) and ν_2^+ of 80 meV of the ion core at the $\tilde{D}\ ^2E$ state are estimated from the spectrum in Figure 4b. The vibrational frequency derivations between the above observations and those of the neutral molecule are due to the structural relaxations of the cation core CCl_3H^+ at the different excited states. Although the scanning step 0.02 eV employed in this work is a little larger, the vibrational structures in bands F3 and F4 are believable because their signal strengths surpass the experimental statistic uncertainties; more importantly, these vibrational fine structures are consistently observed for the minor isotope $^{37}Cl^-$ (see Figure 2). It is noted that the isotope effect on the above vibrational frequencies (the derivations less than 1 meV [39,40]) is too weak to be detected in the present work.

In band F3, two multibody fragmentation channels, $CCl_3H + h\nu \rightarrow CHCl^+ + Cl + Cl^-$ ($E_{threshold}$ = 12.86 eV) and $CCl_3H + h\nu \rightarrow CCl_2^+ + H + Cl^-$ ($E_{threshold}$ = 12.98 eV), also can be accessed (see Figure 3). The energies given in the parentheses are calculated in this work. They are in accord with the predictions using the thermochemical results.[20] Such agreements can also be found for the other new ion-pair dissociation channels listed in Table 1. It is noted that the AEs for $CHCl^+$ (13.94 eV) and CCl_2^+ (12.11 eV) estimated in ref 20 were a little higher or lower than the present $E_{threshold}$ values. Unfortunately, CCl_2^+

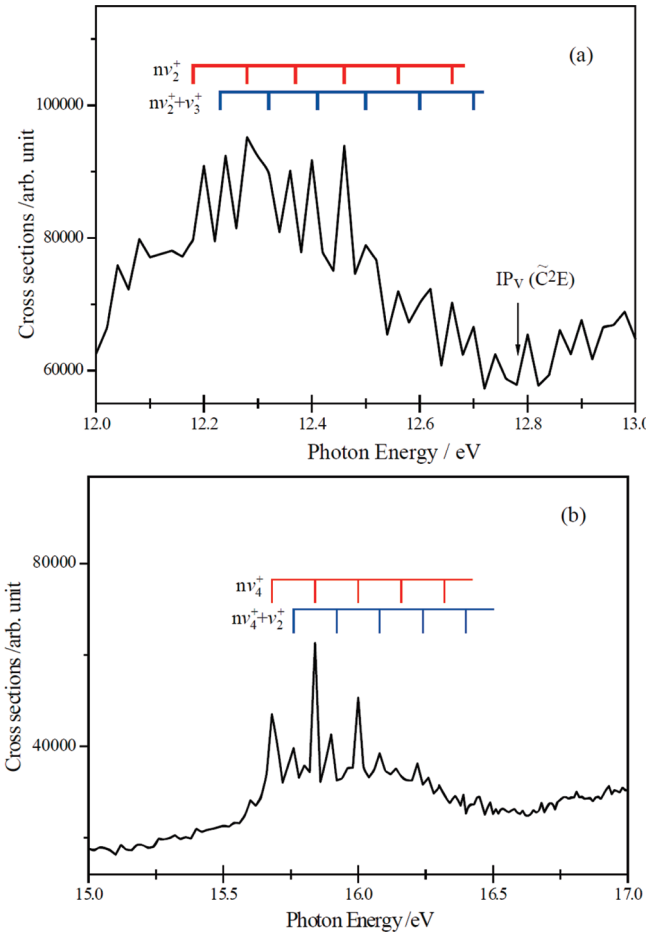

Figure 4. (a) Two series of the vibrational excitations near $\tilde{C}\ ^2E$ ionic state (an arrow pointing to the IP$_v$ value cited from ref [20]). (b) Two series of the vibrational excitations around $\tilde{D}\ ^2E$ ionic state.

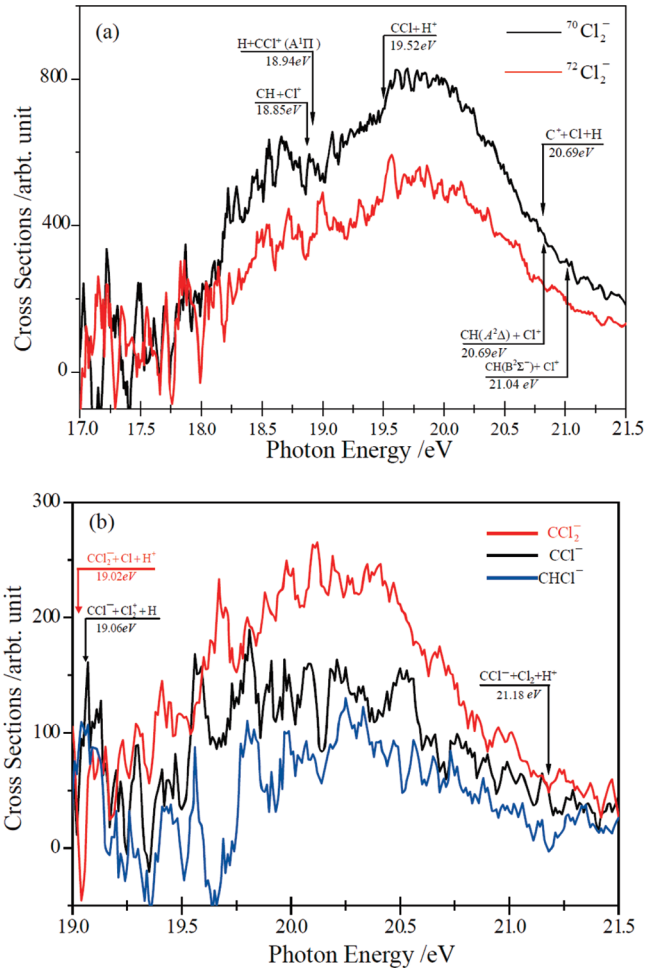

Figure 5. Anion yield spectra for $^{70}Cl_2^-$ and $^{72}Cl_2^-$ (a) and for CCl_2^-, CCl^-, and $CClH^-$ (b).

was not detected in the TPEPICO study;[20] only daughter ion $CHCl_2^+$ was detected several decades ago.[16] According to the thermochemical values, only one ion-pair dissociation channel $CCl_3H + h\nu \rightarrow CCl^+(a^3\Pi_1) + HCl + Cl^-$ ($E_{threshold}$ = 13.78 eV) may be involved in the energy range of 13.00−14.00 eV. It is usually forbidden to produce the triplet state $CCl^+(a^3\Pi_1)$[34] in the single photon absorption, but this ion-pair dissociation channel can be accessed by a transition through a conical cone between the singlet and triplet excited state potential energy surfaces.

In band F4 (14.10−15.00 eV), a small but distinct peak at 14.55 eV can be tentatively assigned with the following cascade processes: the Cl_2 species at the ion-pair excited state $D'2^3\Pi_g$ can be directly produced by the photolysis of CCl_3H, and then this highly excited metastable state decays through ion-pair dissociation $Cl_2(D'2^3\Pi_g) \rightarrow Cl^+ + Cl^-$, which can be induced by the strong pulsed field (field strength ~ 16 500 V/m) employed in our reflectron TOF mass spectrometer.[9,22,23] In the previous vacuum-UV fluorescence spectroscopy study of CCl_3H,[19] the $Cl_2(D'2^3\Pi_g)$ fragment can be produced via the direct photodissociations at the different energies: the threshold of $CCl_3H + h\nu \rightarrow Cl_2(D'2^3\Pi_g) + CClH$ is 11.21 eV, while the thresholds are 14.46 eV of $CCl_3H + h\nu \rightarrow Cl_2(D'2^3\Pi_g) + CH + Cl$ and 14.55 eV of $CCl_3H + h\nu \rightarrow Cl_2\ (D'2^3\Pi_g) + HCl + C$. The $Cl_2(D'2^3\Pi_g)$ species can be further decomposed via the ion-pair dissociation ($Cl^+ + Cl^-$), which is induced with the pulsed field strength of 16 500 V/m. Therefore, plenty of Cl^- ions produced in the above cascade processes, specifically for the latter two pathways yielding $Cl_2(D'2^3\Pi_g)$, can attribute to the band F4 peak (14.55 eV) observed in Figures 2 and 3.

As for the low-energy shoulder of band F5 (15.00−15.70 eV), three multibody fragmentations, $CCl_3H + h\nu \rightarrow Cl + H + CCl^+ + Cl^-$ ($E_{threshold}$ = 15.05 eV), $CCl_3H + h\nu \rightarrow Cl_2 + CH^+ + Cl^-$ ($E_{threshold}$ = 15.45 eV), and $CCl_3H + h\nu \rightarrow CCl + HCl^+ + Cl^-$ ($E_{threshold}$ = 15.65 eV), can be accessed in energy. Two multibody fragmentations, $CCl_3H + h\nu \rightarrow CH + Cl_2^+ + Cl^-$($E_{threshold}$ = 16.30 eV) and $CCl_3H + h\nu \rightarrow CClH + Cl^+ + Cl^-$ ($E_{threshold}$ = 16.37 eV), may be responsible for the high-energy shoulder (around 16.50 eV) of band F5.

With the increase of photon energy, more multibody fragmentations may be involved in the ion-pair dissociations. As shown in Figure 3, five, four, and six multibody fragmentation channels may be responsible for bands F6, F7, and F8, respectively. In Table 1, it is noted that four excited species, CH at A $^2\Delta$, CH at B $^2\Sigma^-$, CCl at A $^2\Delta$, and CCl^+ at A $^1\Pi$, can be produced in the energy range of 18.0−20.0 eV. Some of them may be presented in the fluorescence action spectra for the transitions of CH (A $^2\Delta$, B $^2\Sigma^- \rightarrow$ X $^2\Pi$) and CCl (A $^2\Delta \rightarrow$ X $^2\Pi$),[19] although the productions of CH at A $^2\Delta$ and B $^2\Sigma^-$ and CCl at A $^2\Delta$ via the ion-pair dissociations may be minor contributions. Here, we suggest that the

dx.doi.org/10.1021/jp2000927 |J. Phys. Chem. A 2011, 115, 4248–4254

Table 2. Energetics of Ion-Pair Dissociations for the Minor Negative Fragments

negative ion	ion-pair dissociation channel	dissociation energy/eV
Cl_2^-	$Cl_2^- + C + H + Cl^+$	22.39 [a]
	$Cl_2^- + CH(B\ ^2\Sigma^-) + Cl^+$	21.04 [b]
	$Cl_2^- + H + Cl + C^+$	20.68 [a]
	$Cl_2^- + CH(A\ ^2\Delta) + Cl^+$	20.69 [b]
	$Cl_2^- + CCl + H^+$	19.57 [a]
	$Cl_2^- + H + CCl^+(A\ ^1\Pi)$	18.94 [a]
	$Cl_2^- + CH + Cl^+$	18.90 [a]
	$Cl_2^- + H + CCl^+(a^3\Pi_1)$	16.85 [a]
	$Cl_2^- + Cl + CH^+$	16.57 [a]
	$Cl_2^- + HCl + C^+$	16.25 [a]
	$Cl_2^- + H + CCl^+$	13.69 [a]
	$Cl_2^- + CHCl^+$	11.49 [a]
CCl_2^-	$CCl_2^- + Cl + H^+$	19.02 [a]
	$CCl_2^- + H + Cl^+$	18.39 [a]
	$CCl_2^- + HCl^+$	13.73 [a]
CCl^-	$CCl^- + Cl_2 + H^+$	21.18 [a]
	$CCl^- + H + Cl_2^+$	19.06 [a]
	$CCl^- + HCl + Cl^+$	18.60 [a]
	$CCl^- + Cl + HCl^+$	18.38 [a]
$CHCl^-$	$CHCl^- + Cl + Cl^+$	18.77 [a]
	$CHCl^- + Cl_2^+$	14.81 [a]

[a] Calculated in this work. [b] Estimated using the thermochemical data from ref 19.

ion-pair dissociations at the high photon energies could be another pathway to produce the excited-state fragments, except for the neutral fragmentations and ionization photodissociations. It is noted that we could not exhaust all possible multibody fragmentation channels, in particular, at the excited-state potential energy surfaces, to produce Cl^- as well as the following anionic species.

Thermochemistry of Cl_2^-, CCl^-, CCl_2^-, and $CClH^-$. See Figure 5a; we will not go into the details about the spectral structures either for $^{70}Cl_2^-$ or $^{72}Cl_2^-$ in the energy range of 17.00−18.20 eV due to the large experimental uncertainty. The spectra of $^{70}Cl_2^-$ and $^{72}Cl_2^-$ show similar fine structures in the energy range of 18.30−21.00 eV. In general, there are the highest intensities around 19.80 eV and the shoulders at 18.70 eV. $^{74}Cl_2^-$ signals are too low to obtain the efficiency curve.

In Table 2, the energetic values of 12 possible dissociation channels producing Cl_2^- (here we only consider the predominant isotope ^{35}Cl) are listed. The AE value of Cl_2^- should be 11.49 eV, corresponding to $CCl_3H + h\nu \rightarrow Cl_2^- + CHCl^+$. However, the much lower signals of Cl_2^- cannot enable us to determine this threshold. Only six channels to Cl_2^- can be accessed in the photon energy shown in Figure 5a. The energetic values of three, four, and two ion-pair dissociations are presented for CCl_2^-, CCl^-, and $CClH^-$, respectively. Due to the low signal strengths and the large uncertainties at the lower energies, the IPAES for CCl_2^-, CCl^-, and $CClH^-$ are shown in Figure 5b only in the photon energy range of 19.00−21.50 eV. The signal strengths of CCl_2^- are a little stronger than the other two. Besides the dissociations considered in Table 2 and some of them assigned in Figure 5b, in this energy range the electron transitions from the inner valence orbital $2a_1$ (of the character Cl 2p lone pair) to the high-lying excited states, e.g., Rydberg series converging to $\tilde{F}\ ^2A_1$ (IP_v = 20.65 eV), may also be involved in the ion-pair dissociations.

4. CONCLUSION

Negative ions Cl^-, Cl_2^-, CCl^-, CCl_2^-, $CHCl^-$, and their isotope species are observed for the first time in the ion-pair photodissociations of CCl_3H in the energy range of 10.00−21.50 eV. The fragmentation enthalpies for Cl^-, Cl_2^-, CCl^-, $CHCl^-$, and CCl_2^- are estimated with the thermochemistry data available in the literature, and some of these ion-pair dissociations are tentatively assigned in the anion yield spectra. The spectra of two isotopes $^{35}Cl^-$ and $^{37}Cl^-$ show some additional peaks arising from the energetically accessible multibody fragmentations, besides the strong bands corresponding to the electron transitions from valence to Rydberg states converging to the molecular ionic states. In the spectrum of Cl^-, a distinct peak at 14.55 eV may be due to such cascade processes, namely, the Cl^- anions result from the pulsed field induced ion-pair dissociation of Cl_2 at the excited state ($D'2^3\Pi_g$) which is produced in the photodissociation of CCl_3H. Two vibrational excitation progressions, $n\nu_2^+$ and $n\nu_2^+ + \nu_3^+$, and $n\nu_4^+$ and $n\nu_4^+ + \nu_2^+$, are observed around $\tilde{C}\ ^2E$ and $\tilde{D}\ ^2E$ ionic states, respectively.

AUTHOR INFORMATION

Corresponding Author
*E-mail: sxtian@ustc.edu.cn.

ACKNOWLEDGMENT

This work is supported by NSFC (Grant Nos. 10775130 and 10979048), MOST (Grant No. 2007CB815204), USTC-NSRL association funding, and the Fundamental Research Funds for the Central Universities (Grant No.WK2340000012).

REFERENCES

(1) Berkowitz, J. In *VUV and Soft-Ray Photoionization*; Becker, U., Shirley, D. A., Eds.; Plenum: New York, 1996; p 263.
(2) Suits, A. G.; Hepburn, J. W. *Annu. Rev. Phys. Chem.* **2006**, *57*, 431.
(3) Scully, S. W.; Mackie, J. R. A.; Browning, R.; Dunn, K. F.; Latimer, C. J. *Phys. Rev. A* **2004**, *70*, No. 042707.
(4) Mistuke, K.; Hottori, H.; Yoshita, H. *J. Chem. Phys.* **1993**, *99*, 6642.
(5) Suzuki, S.; Mistuke, K.; Imamura, T.; Koyano, I. *J. Chem. Phys.* **1992**, *96*, 7500.
(6) Simpson, M. J.; Tuckett, R. P.; Dunn, K. F.; Hunniford, C. A.; Latimer, C. J. *J. Chem. Phys.* **2009**, *130*, 194302.
(7) Simpson, M. J.; Tuckett, R. P. *J. Phys. Chem. A* **2010**, *114*, 8043.
(8) Shaw, D. A.; Holland, D. M. P.; Walker, I. C. *J. Phys. B* **2006**, *39*, 3549.
(9) Tian, S. X.; Xu, Y. F.; Wang, Y. F.; Feng, Q.; Chen, L. L.; Sun, J. D.; Liu, F. Y.; Shan, X. B.; Sheng, L. S. *Chem. Phys. Lett.* **2010**, *496*, 254.
(10) Dehmer, P. M.; Chupka, W. A. *J. Chem. Phys.* **1975**, *62*, 4525.
(11) Aucott, M. L.; McCulloch, A.; Graedel, T. E.; Kleiman, G.; Migdeley, P.; Li, Y. F. *J. Geophys. Res., [Atmos.]* **1999**, *104* (D7), 8405.
(12) Khalil, M. A. K.; Moore, R. M.; Harper, D. B.; Lobert, J. M.; Erickson, D. J.; Koropalov, V.; Sturges, W. T.; Keene, W. C. *J. Geophys. Res.* **1999**, *104*, 8333.
(13) Yang, X. F.; Felder, P.; Huber, J. R. *Chem. Phys.* **1994**, *189*, 127.
(14) Lee, L. C.; Suto, M. *Chem. Phys.* **1987**, *114*, 423.
(15) Denifl, S.; Mauracher, A.; Sulzer, P.; Bacher, A.; Märk, T. D.; Scheier, P. *Int. J. Mass Spectrom.* **2007**, *265*, 139.
(16) Werner, S.; Tsai, B. P.; Baer, T. *J. Chem. Phys.* **1974**, *60*, 3650.
(17) Potts, A. W.; Lempka, H. J.; Streets, D. G.; Price, W. C. *Philos. Trans. R. Soc. London, Ser. A* **1970**, *59*, 268.
(18) von Niessen, W.; Asbrink, L.; Bieri, G. *J. Electron Spectrosc. Relat. Phenom.* **1982**, *26*, 173.

(19) Seccombe, D. P.; Tuckett, R. P.; Baumgärtel, H.; Jochims, H. W. *Phys. Chem. Chem. Phys.* **1999**, *1*, 773.
(20) Seccombe, D. P.; Chim, R. Y. L.; Jarvis, G. K.; Tuckett, R. P. *Phys. Chem. Chem. Phys.* **2000**, *2*, 769.
(21) Rogers, N. J.; Simpson, M. J.; Tuckett, R. P.; Dunn, K. F.; Latimer, C. J. *Phys. Chem. Chem. Phys.* **2010**, *12*, 10971.
(22) Feng, Q.; Tian, S. X.; Zhao, Y. J.; Liu, F. Y.; Shan, X. B.; Sheng, L. S. *Chin. Phys. Lett.* **2009**, *26*, 053402.
(23) Feng, Q.; Xu, Y. F.; Sun, J. D.; Tian, S. X.; Liu, F. Y.; Shan, X. B.; Sheng, L. S. *Chin. Phys. Lett.* **2009**, *26*, 103401.
(24) Traeger, J. C.; McLoughlin, R. G. *J. Am. Chem. Soc.* **1981**, *103*, 3647.
(25) Chase, M. W. *J. Phys. Chem. Ref. Data Monogr.* **1998**, 9.
(26) Lias, S. G.; Bartmess, J. E.; Liebman, J. F.; Holmes, J. L.; Lerin, R. D.; Mallard, W. G. *J. Phys. Chem. Ref. Data Suppl.* **1988**, *17*, 1.
(27) Li, J.; Hao, Y. S.; Yang, J.; Zhou, C.; Mo, Y. X. *J. Chem. Phys.* **2007**, *127*, 104307.
(28) Yencha, A. J.; Cormack, A. J.; Donovan, R. J.; Hopkirk, A.; King, G. C. *Chem. Phys.* **1998**, *238*, 109.
(29) Bowen, K. H.; Liesegang, G. W.; Sanders, R. A.; Herschbach, D. W. *J. Phys. Chem.* **1983**, *87*, 557.
(30) Schwartz, R. L.; Davico, G. E.; Ramond, T. M.; Lineberger, W. C. *J. Phys. Chem. A* **1999**, *103*, 8213.
(31) Reid, C. J. *Chem. Phys.* **1996**, *210*, 501.
(32) Gilles, M. K.; Ervin, K. M.; Ho, J.; Lineberger, W. C. *J. Phys. Chem.* **1992**, *96*, 1130.
(33) Jacox, M. E. *J. Phys. Chem. Ref. Data Monogr.* **1994**, 3.
(34) Tsuji, M.; Mizuguchi, T.; Shinohara, K.; Nishimura, Y. *Can. J. Phys.* **1983**, *61*, 838.
(35) Martin, J. D. D.; Hepburn, J. W. *J. Chem. Phys.* **1998**, *109*, 8139.
(36) Grisogono, A. M.; Pascual, R.; von Nissen, W.; Weigold, E. *Chem. Phys.* **1989**, *135*, 317.
(37) Jadrny, R.; Karlsson, L.; Mattsson, L.; Siegbahn, K. *Phys. Scr.* **1977**, *16*, 235.
(38) Shimanouchi, T. *Tables of Molecular Vibrational Frequencies Consolidated*, Vol. I; National Bureau of Standards: Gaithersburg, MD, 1972; pp 1−160.
(39) Fuss, W.; Weizbauer, S. *Ber. Bunsen-Ges. Phys. Chem.* **1995**, *99*, 289.
(40) Ruoff, A.; Bürger, H. *Spectrochim. Acta, Part A* **1970**, *26*, 989.